

VLBI observations of the most radio-loud, narrow-line quasar SDSS J094857.3+002225

Akihiro DOI,^{1,2,3} Hiroshi NAGAI,^{4,3} Keiichi ASADA,³
 Seiji KAMENO,^{5,3} Kyoaki WAJIMA,⁶ and Makoto INOUE³

¹Department of Physics, Faculty of Science, Yamaguchi University,
 Yoshida, Yamaguchi, Yamaguchi 753-8512

²Department of Astronomy, Faculty of Science, The University of Tokyo,
 7-3-1 Hongo, Bunkyo-ku, Tokyo 113-0033, Japan

³National Astronomical Observatory, 2-21-1 Osawa, Mitaka, Tokyo 181-8588, Japan

⁴Department of Astronomical Science, The Graduate University for Advanced Studies,
 2-21-1 Osawa, Mitaka, Tokyo 1811-8588, Japan

⁵Department of Physics, Faculty of Science, Kagoshima University,
 1-21-35 Korimoto, Kagoshima 890-0065

⁶Korea Astronomy and Space Science Institute,
 61-1 Whaam-dong, Yuseong, Daejeon 305-348, Korea

(Received 2006 February 28; accepted 2006 August 24)

Abstract

We observed the narrow-line quasar SDSS J094857.3+002225, which has the highest known radio loudness for a narrow-line Seyfert 1 galaxy (NLS1), at 1.7–15.4 GHz with the Very Long Baseline Array (VLBA). This is the first very-long-baseline interferometry (VLBI) investigation for a radio-loud NLS1. We independently found very high brightness temperatures from (1) its compactness in a VLBA image and (2) flux variation among the VLBA observation, our other observations with the VLBA, and the Very Large Array (VLA). A Doppler factor larger than 2.7–5.5 was required to meet an intrinsic limit of brightness temperature in the rest frame. This is evidence for highly relativistic nonthermal jets in an NLS1. We suggest that the Doppler factor is one of the most crucial parameters determining the radio loudness of NLS1s. The accretion disk of SDSS J094857.3+002225 is probably in the very high state, rather than the high/soft state, by analogy with X-ray binaries with strong radio outbursts and superluminal jets such as GRS 1915+105.

Key words: galaxies: active — galaxies: jets — galaxies: Seyfert — quasars: individual(SDSS J094857.3+002225) — radio continuum: galaxies

1. Introduction

Narrow-line Seyfert 1 galaxies (NLS1s; Osterbrock & Pogge 1985; Pogge 2000) are usually found as radio-quiet objects (Zhou & Wang 2002). Various properties observed through optical and X-ray bands suggest that NLS1s are active galactic nuclei (AGNs) of highly accreting ($L_{\text{bol}}/L_{\text{Edd}} \sim 1$, where L_{bol} and L_{Edd} are bolometric and Eddington luminosities, respectively) systems (e.g., Pounds et al. 1995; Boroson 2002). The radio-quietness of NLS1s may be related to the suppression of radio jets emanated from accretion disks with high accretion rates (Greene et al. 2006), as well as the disks of X-ray binaries in the *high/soft* state (see, e.g., McClintock & Remillard 2003 for a review).

On the other hand, radio-loud NLS1s do exist, although they are very rare (Zhou & Wang 2002). There is no significant difference between radio-quiet and radio-loud NLS1s in optical and X-ray properties (SDSS J094857.3+002225, Zhou et al. 2003; RX J0134.2–4258, Grupe et

al. 2000; RGB J0044+193, Siebert et al. 1999; PKS 2004–447, Oshlack et al. 2001; PKS 0558–504, Wang et al. 2001). The origin of the radio excess of the radio-loud NLS1s has been unknown. Hardening of X-ray spectra during rapid X-ray flares of the radio-loud NLS1 PKS 0558–504 in a few minutes could arise from transient spectral dominance of synchrotron emission from relativistically boosted jets (Wang et al. 2001) similar to radio-loud quasars (e.g., Reeves et al. 1997). However, properties of radio jets in NLS1s are slightly known. Their linear sizes are $\lesssim 300$ pc (Ulvestad et al. 1995), which correspond to ~ 1 arcsec resolutions of connected interferometries; there are only a few images that have been obtained by very-long-baseline interferometry (VLBI) observations (Lal et al. 2004; Middelberg et al. 2004).

We started VLBI-imaging several NLS1s. SDSS J094857.3+002225 was discovered at $z = 0.584$ in the Sloan Digital Sky Survey (SDSS) early data release (Williams et al. 2002). With $\text{FWHM}(\text{H}\beta) \approx 1500 \text{ km s}^{-1}$ and undetected [OIII] lines, this source was consistent

Table 1. Parameters of observations.

Date	Array	ν_c (GHz)	$\Delta\nu$ (MHz)	pol.	$t_{\text{scan}} \times N_{\text{scan}}$
(1)	(2)	(3)	(4)	(5)	(6)
2003Oct30	VLBA	15.365	32	L	46×52
		8.421	32	R	35×18
		4.987	32	L	56×7
		2.271	32	R	85×6
		1.667	32	L	94×6
		1.667	32	L	46×12
2005May09	VLBA	14.94	100	dual	43×2
		8.460	100	dual	33×1
		4.860	100	dual	33×1
		1.425	100	dual	43×1

Col. (1) observation date; Col. (2) array; Col. (3) center frequency; Col. (4) bandwidth; Col. (5) polarization. L and R denote left and right circular polarization, respectively; Col. (6) scan lengths × number of scans.

with the conventional definition of NLS1s (Zhou et al. 2003). Its radio counterpart was found in the Faint Images of the Radio Sky at Twenty-centimeter (FIRST) survey (Becker et al. 1995). This has been the most radio-loud ($R \approx 2000$) object in NLS1s (Zhou et al. 2003), where R is “radio loudness” conventionally defined as the ratio of 6 cm radio to B -band flux densities with a threshold of $R = 10$ separating radio-loud and radio-quiet objects (e.g., Visnovsky et al. 1992; Stocke et al. 1992; Kellermann et al. 1994). Zhou et al. (2003) suggested that its rapid (\sim years) radio-flux variations were caused by relativistic boosting of a jet. This is appropriate for the first target of VLBI observations, because of the brightest (~ 300 mJy) NLS1 in radio bands. In the present paper, we report VLBI observations in milliarc-second (mas) resolutions for SDSS J094857.3+002225; this is the first VLBI study for a radio-loud NLS1. Throughout this paper, a flat cosmology is assumed, with $H_0 = 71 \text{ km s}^{-1} \text{ Mpc}^{-1}$, $\Omega_M = 0.27$, and $\Omega_\Lambda = 0.73$ (Spergel et al. 2003). Therefore, 1 mas corresponds to 6.6 pc at the distance to SDSS J094857.3+002225. Its optical magnitude m_B (SDSS) ≈ 18.89 mag (Zhou et al. 2003) corresponding to $M_B = -23.8$ mag implies that this source is a quasar rather than a Seyfert galaxy according to the standard definition of a quasar, $M_B < -23$ mag.

2. Observations and data reduction

We observed SDSS J094857.3+002225 using ten stations of the Very Long Baseline Array (VLBA) on October 30, 2003 and May 09, 2005. The observation parameters are shown in Table 1. Standard procedures were applied for data reduction using the Astronomical Image Processing System (AIPS; Greisen 2003). Amplitude calibration used a priori gain values, together with system temperatures measured during the observations, and was typically 5% accurate. Imaging, deconvolution, and self-calibration for phase and amplitude were performed using the Difmap software (Shepherd 1997). The final self-calibration in phase was done at all the frequencies with a

solution interval of 10 s, which is much less than coherence times.

SDSS J094857.3+002225 was also observed in a snapshot mode with the Very Large Array (VLA) B-array configuration on December 15, 2003. The VLA observations were carried out in good weather conditions. Data were calibrated using the AIPS, according to the standard manner. Maps in Stokes I were made, and deconvolution and self-calibration were performed in the AIPS. A solution interval of 10 s, similar to the VLBA data reduction, was used in self-calibration to correct of visibility phases. The flux-scaling factors of visibility amplitude were determined by observations from the standard calibrator 3C 48, with an uncertainty of $\sim 3\%$.

3. RESULTS

3.1. VLBA images

In the VLBA data analyses, source structure models were established by visibility-based model fitting with point and/or elliptical-Gaussian profile(s) in the Difmap. Here, we describe the results of the fitting, particularly at 15 GHz, where the highest spatial resolution was available during the observations. The free parameters were flux density and two-dimensional position for a point source model, along with major axis, axis ratio, and position angle of the axis for an elliptical-Gaussian model.

One point source resulted in $\chi^2/\text{dof} = 77821/57109$; adding one more point source showed $\chi^2/\text{dof} = 73870/57106$: a dramatic improvement of $\Delta\chi^2/\Delta\text{dof} = 3950/3$, which is significant at $>99.9\%$ confidence. We found both a strong component “C0” and a weak component “C1,” not only at 15 GHz but also at 5 and 8.4 GHz. However, the two components were not separable from each other at 1.7 and 2.3 GHz, where the resolution was poorer (Table 2 and Fig. 1). No other significant emission in the residual images was found. We had initially suspected that the weaker component was created by a deconvolution error, because the separation was the same as or smaller than the synthesized beams. However, a

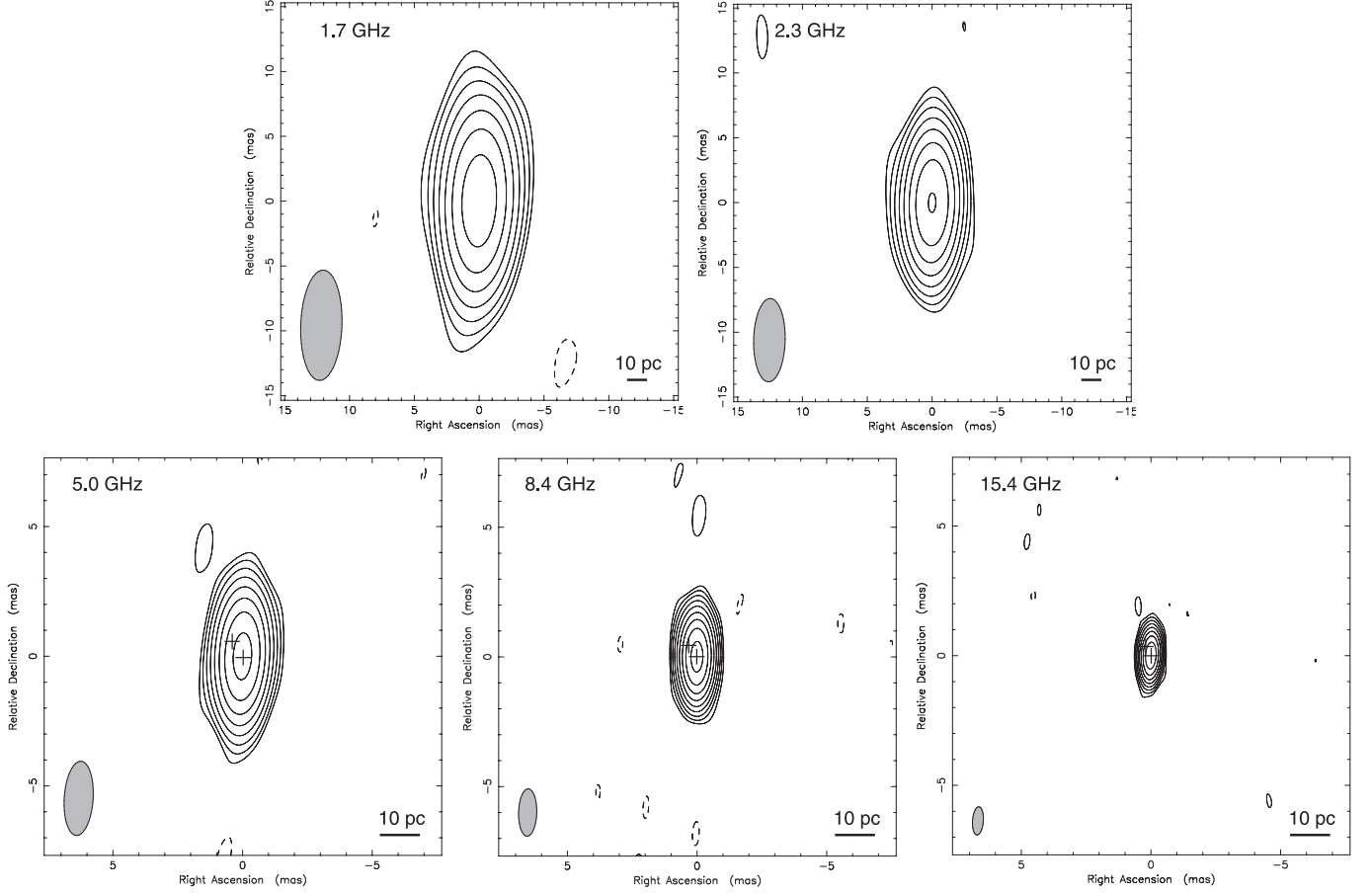


Fig. 1. VLBA contour maps of SDSS J094857.3+002225 on Oct 30, 2003. The contour levels are $3\sigma \times -1, 1, 2, 4, 8, 16, 32, 64, 128$, and 256 , where σ is the RMS of image noise at each frequency. In the images at 5.0, 8.4, and 15.4 GHz, “+” symbols represent the positions of C0 and C1 components, which were identified by visibility-based model fitting (Section 3.1).

number of test images from fake visibility data created by Monte-Carlo simulations with an identical (u, v) -coverage and a similar sensitivity indicate that a strong component and a weak one that are separated by >0.10 mas at $PA=30^\circ$ can be clearly resolved from each other. We are confident, therefore, in the existence of the two components separated by 0.41 mas at 15 GHz. Although the separations between C0 and C1 were different at observing frequencies, the position angles of C1 from C0 were consistent (Table 2).

Furthermore, we attempted to fit the visibility data with two elliptical Gaussians. However, this attempt failed because the source sizes were too small. To evaluate how a large source can be resolved in the VLBA observation, we made imaging simulations in the same manner using fake visibility data that were made by combining a strong circular-Gaussian source of 461 mJy with various diameters and a weak point source of 21 mJy separated by 0.4 mas at $PA \sim 30^\circ$ (see similar analyses in Taylor et al. 2004). These tests suggest that the stronger source can be clearly resolved if the given size is >0.05 mas in diameter. The VLBA observation should have the ability to resolve a size of ~ 0.10 mas for the stronger component. The size of 0.10 mas corresponds to a decrease of $\sim 10\%$ in visibility amplitude at the longest baseline of the VLBA

at 15 GHz. Because of the sufficiently good sensitivity and calibration, we were able to determine the fringe visibility to 5% (see similar discussion by Kellermann et al. 1998). Thus, we assume the effective resolution of our VLBA observation at 15 GHz is around 0.10 mas, which is about quarter of the synthesized beam. The component C0 is presumably compact with a size of < 0.10 mas, corresponding to < 0.66 pc on a linear scale.

3.2. VLA images

In the VLA images, only a single, unresolved component was found at all the frequencies, except for 1.4 GHz, where radio interference affected the data. No diffuse emission component was found, even in (u, v) -tapered images. Flux density was measured by Gaussian model fitting on the image domain using the task JMFIT of the AIPS.

3.3. Measured flux densities

Measured flux densities are listed in Table 2. We estimated the total error from the root sum square of the uncertainty of amplitude calibration and the error in Gaussian fitting (including thermal noise).

The total spectra of observed VLBA flux densities were slightly inverted ($\alpha > 0$, $S_\nu \propto \nu^{+\alpha}$), which is consistent with past observations. Non-simultaneous observations

Table 2. Observational results.

ν (GHz)	Comp. (1)	S_ν (mJy) (2)	σ_{rms} (mJy beam $^{-1}$) (4)	θ_{maj} (arcsec) (5)	θ_{min} (arcsec) (6)	PA (deg) (7)	$l(\text{C0-C1})$ (mas) (8)	$PA(\text{C0-C1})$ (deg) (9)
VLBA observed on Oct 30, 2003								
15.365L	C0	461.3 \pm 23.1	0.65	0.0011	0.0004	-3.3
	C1	20.6 \pm 1.6	0.41 \pm 0.02	+30.7
8.421R	C0	363.0 \pm 18.2	0.37	0.0019	0.0008	-2.7
	C1	25.2 \pm 1.4	0.51 \pm 0.01	+34.9
4.987L	C0	258.9 \pm 13.0	0.56	0.0031	0.0012	-3.8
	C1	32.0 \pm 2.4	0.75 \pm 0.02	+33.1
2.271R	...	245.4 \pm 12.3	0.67	0.0072	0.0029	-2.8
1.667L	...	173.0 \pm 8.7	0.55	0.0098	0.0040	+0.9
VLBA observed on May 09, 2005								
1.667L	...	85.7 \pm 4.4	0.58	0.0104	0.0039	-1.4
VLA-B observed on Dec 15, 2003								
14.94	...	334.1 \pm 10.1	0.56	0.9	0.4	-48.1
8.460	...	359.8 \pm 10.8	0.36	1.8	0.7	-50.3
4.860	...	304.7 \pm 9.7	1.89	3.0	1.2	-49.9
1.425	...	176.6 \pm 6.0	1.53	9.3	4.2	-50.6

Col. (1) observing frequency. L and R denote left and right circular polarization, respectively; Col. (2) component name. C0 and C1 denote the bright and weaker component, respectively, which were spatially resolved by visibility-based model fitting (Section 3.1); Col. (3) flux density; Col. (4) RMS of image noise; Col. (5) FWHM of synthesized beam at major axis; Col. (6) at minor axis; Col. (7) position angle of synthesized beam; Col. (8) separation between C0–C1; Col. (9) position angle of C1 from C0.

from 111.5 mJy at 1.4 GHz by the FIRST survey (Becker et al. 1995) and 234 mJy at 8.4 GHz by the Jodrell Bank VLA Astrometric Survey (Browne et al. 1998) showed an inverted spectrum. Simultaneous observations at 2.7, 5, and 10.7 GHz (Reich et al. 2000) showed a spectral index, $\alpha = -0.24 \pm 0.08$. Our VLA flux densities were consistent with or less than those of the VLBA; this suggests that there is no missing flux in the VLBA images of this object.

The VLBA flux density at 1.7 GHz decreased to 50% in 19 months. The flux density at 15 GHz also decreased to 69% in 46 days between the VLBA and VLA observations. We believe that these were intrinsic decreases of flux density rather than losses of high-frequency coherence on the VLA data. The VLA observations were made in good weather conditions. The coherence loss should be inhibited to the same level as that of the VLBA, since a sufficiently short solution interval, 10 s, was adopted for phase self-calibration to both the VLBA and VLA data (Section 2).

4. Discussion

4.1. Very high brightness temperatures

We can derive brightness temperatures from both the VLBA image and the flux variability. Using imaging analysis, brightness temperature in the rest frame is calculated using (cf. Lähteenmäki et al. 1999)

$$T_{\text{Brest}}(\text{img}) = \frac{1+z}{\delta} \frac{c^2 S_{\nu \text{obs}}^{\text{obs}}}{2k_{\text{B}} \nu_{\text{obs}}^2 (\theta_{\text{obs}}/2)^2 \pi}, \quad (1)$$

where c is the speed of light, k_{B} is the Boltzmann constant, S_ν is the flux density at frequency ν , θ is the

angular diameter of a source, and suffixes of “obs” and “rest” denote quantities in the observer frame and the rest frame, respectively. The Doppler factor is defined as $\delta \equiv \sqrt{1 - \beta^2}/(1 - \beta \cos \phi)$, where $\beta \equiv v/c$ (v is the source speed), and ϕ is the “viewing angle” between the direction of the source velocity and our line of sight. Given an apparent diameter of <0.10 mas for C0 in the 15-GHz VLBA data (Section 3.1), $T_{\text{Brest}}(\text{img}) > 5.5 \times 10^{11}/\delta$ K.

Alternatively, with flux variation, a brightness temperature in the rest frame can be calculated independently using (cf. Lähteenmäki et al. 1999)

$$T_{\text{Brest}}(\text{var}) > \frac{1+z}{\delta^3} \frac{D_{\text{co}}^2 \Delta S_{\nu \text{obs}}^{\text{obs}}}{2\pi k_{\text{B}} \nu_{\text{obs}}^2 (\Delta t_{\text{obs}})^2}, \quad (2)$$

where D_{co} is the comoving distance, $\Delta S_{\nu \text{obs}}^{\text{obs}}$ is a change of observed flux density in a period, of Δt_{obs} . In this equation, we assume exponential decay as seen in radio outbursts in blazars (Valtaoja et al. 1999). We found that the flux density decreases by 31% in 46 days at 15 GHz, and by 50% in 19 months at 1.7 GHz (Section 3.3), which implies that $T_{\text{Brest}}(\text{var}) > 3.3 \times 10^{13}/\delta^3$ K and $T_{\text{Brest}}(\text{var}) > 1.1 \times 10^{13}/\delta^3$ K, respectively. A very high brightness temperature in this source has also been suggested by Zhou et al. (2003) from 1.4-GHz flux variation in \sim years time scale. These very high brightness temperatures form clear evidence for a nonthermal process in the central engine of this NLS1.

4.2. Highly relativistic jets

Based on near equipartition of energies between radiating particles and a magnetic field, the brightness temperature of nonthermal radio emission should be within a

physically realistic upper limit of $\sim 2 \times 10^{11}$ K in the rest frame (Readhead 1994). Therefore, the Doppler factor should be $\delta > 2.7\text{--}5.5$ for the observed brightness temperatures (Section 4.1). The observed radio emissions are presumably from highly relativistic jets and are enhanced by Doppler boosting. The jets should approach us with a viewing angle of $\theta < 22^\circ$ and a speed of $\beta > 0.76$ for $\delta > 2.7$ (Section 4.1). C1, spatially resolved in the VLBA data (Section 3.1), may be one of the expanding jet components.

Because of the very high brightness temperature, synchrotron self-absorption could be a possible explanation for the inverted spectrum as observed. We show an example of spectral model fitting to the observed VLBA total fluxes using power-law spectra with a low-frequency cut-off due to synchrotron self-absorption: $S_\nu = S_{\nu_0} \nu^{2.5} [1 - \exp(-\tau \nu^{\alpha_0 - 2.5})]$, where S_{ν_0} is a scaling constant, τ is the optical depth, and α_0 is the intrinsic (not absorbed) spectral index. Spectral model fitting was performed on the assumptions that the observed spectrum of C0 is caused by a superposition of self-absorbed synchrotron spectra of two components, and that the observed spectrum of C1 can be represented by a single power-law spectrum. As a result, C0 consists of two convex spectra with peak frequencies at ~ 16 GHz (“C0A”) and ~ 3 GHz (“C0B”), as shown in Fig. 2. The Doppler boosting can be responsible for such high frequencies of the spectral peaks, since $\nu_{\text{obs}} = [\delta/(1+z)]\nu_{\text{rest}}$. The intrinsic peak frequencies could be at several hundreds of MHz. Such high-frequency peaked spectra are reminiscent of those of the Seyfert galaxy III Zw 2 with two compact radio components and an inverted high-frequency spectrum in total flux (Falcke et al. 1999). These components in III Zw 2 are also highly relativistic jets (Brunthaler et al. 2000).

4.3. Implications of SDSS J094857.3+002225

Our observations showed a slightly inverted spectrum at ~ 5 GHz and $R \approx 2530$, which is derived from $m_B(\text{SDSS}) \approx 18.89$ mag (Zhou et al. 2003) and the VLBA total flux density at 5 GHz. Given $\delta > 5.5$ (Section 4.1), the peak frequency of C0A, ~ 16 GHz, should be < 2.9 GHz before Doppler beaming. In the case where $\alpha = -0.6$, a flux density should be amplified by a factor of > 462 from an intrinsic spectrum at the same frequency. Therefore, there is a possibility that SDSS J094857.3+002225 is a radio-quiet object with a steep spectrum in the rest frame, like typical NLS1s (Moran 2000; Zhou & Wang 2002; Ulvestad et al. 1995).

Flat or inverted radio spectra have also been found in the other radio-loud NLS1s, e.g., RGB 0044+193 (Siebert et al. 1999), 2E 1640+5345, RXS J16290+4007, and RX J16446+2619 (Zhou & Wang 2002). Doppler boosting may be responsible for their spectra and radio loudness as well as those of SDSS J094857.3+002225. The observed optical and X-ray properties and black-hole masses of radio-loud NLS1s are not significantly different from those of radio-quiet ones (e.g., Siebert et al. 1999; Wang et al. 2001). From our observations, we suggest that the Doppler factor is a crucial parameter determining the ra-

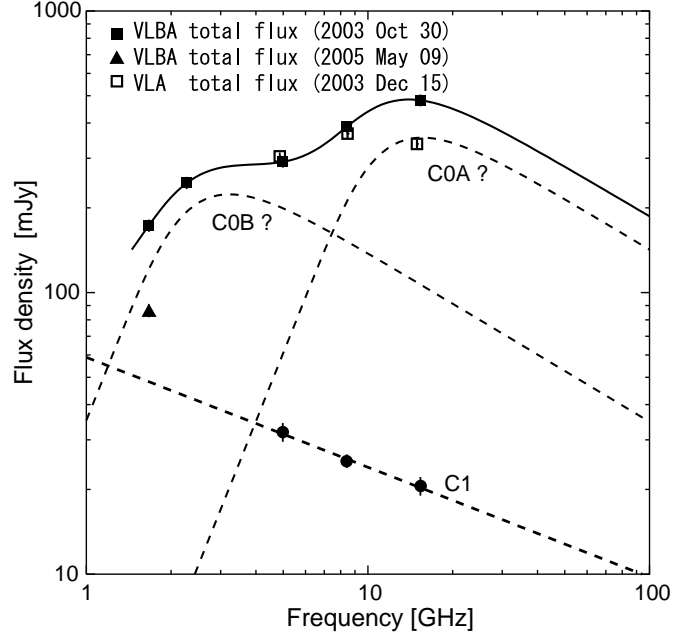


Fig. 2. Radio continuum spectra of SDSS J094857.3+002225. Symbols representing total flux densities are identified in top corner. Filled circles particularly describe the flux densities for component C1. The solid curve represents the spectral model that was determined by spectral model-fitting to the VLBA total fluxes using two self-absorbed synchrotron spectra (“C0A” and “C0B” as dashed curves) with an intrinsic spectral index of $\alpha_0 = -0.6$ and one simple power-law spectrum (C1 as a dashed line). The spatially single component C0 was divided into two spectrally separate components, C0A and C0B with peak frequencies of ~ 16 and 3 GHz, respectively. See Section 4.2 for details.

dio loudness of NLS1s: at least some of NLS1s could possess the ability to generate highly relativistic jets.

Analogies have been drawn between X-ray binaries and AGNs (e.g., Maccarone et al. 2003). NLS1s are thought to be AGNs with high accretion rates. Although X-ray binaries in the *high/soft* state with accretion rates of $L/L_{\text{Edd}} \sim 0.03\text{--}0.1$ have no relevance to jets, strong radio flares have been seen during the *very high* state, which is thought to be a disk in $L/L_{\text{Edd}} > 0.1$, such as GRS 1915+105, with highly relativistic jets (e.g., Fender 2003). SDSS J094857.3+002225 has the potential to be compatible with the *very high* state, rather than the *high/soft* state. Radio-loud NLS1s will be appropriate targets to investigate for the *very high* state on super-massive black hole systems.

5. Summary

Our VLBA and VLA observations have revealed that SDSS J094857.3+002225, which shows the highest known radio loudness for an NLS1, has (1) significant variability on time scales of 46 days and 19 months, (2) an inverted spectrum, and (3) multiple components with a size < 0.10 mas. The derived brightness temperatures were significantly higher than the intrinsic limit, implying

Doppler-beaming with a Doppler factor $\delta > 2.7\text{--}5.5$ and, therefore, relativistic jets. At least some NLS1s could be able to generate highly relativistic jets. We suggest that the Doppler factor is a crucial parameter determining the radio loudness of NLS1s. On the analogy of X-ray binaries, SDSS J094857.3+002225 is probably equivalent to an AGN in the *very high* state rather than the *high/soft* state, because of the highly relativistic jets.

The VLBA and VLA are operated by the National Radio Astronomy Observatory (NRAO), a facility of the National Science Foundation operated under cooperative agreement by Associated Universities, Inc. This research has made use of NASA Astrophysics Data System (ADS) bibliographic services. We thank the referee for suggestions that helped considerably in clarifying the paper.

References

Becker, R. H., White, R. L., & Helfand, D. J. 1995, ApJ, 450, 559

Boroson, T. A. 2002, ApJ, 565, 78

Browne, I. W. A., Wilkinson, P. N., Patnaik, A. R., & Wrobel, J. M. 1998, MNRAS, 293, 257

Brunthaler, A., et al. 2000, A&A, 357, L45

Falcke, H., et al. 1999, ApJL, 514, L17

Fender, R. 2003, ArXiv Astrophysics e-prints, arXiv:astro-ph/0303339

Greene, J. E., Ho, L. C., & Ulvestad, J. S. 2006, ApJ, 636, 56

Greisen, E. W. 2003, Information Handling in Astronomy - Historical Vistas, 109

Grupe, D., Leighly, K. M., Thomas, H.-C., & Laurent-Muehleisen, S. A. 2000, A&A, 356, 11

Kellermann, K. I., Sramek, R. A., Schmidt, M., Green, R. F., & Shaffer, D. B. 1994, AJ, 108, 1163

Kellermann, K. I., Vermeulen, R. C., Zensus, J. A., & Cohen, M. H. 1998, AJ, 115, 1295

Lähteenmäki, A., Valtaoja, E., & Wiik, K. 1999, ApJ, 511, 112

Lal, D. V., Shastri, P., & Gabuzda, D. C. 2004, A&A, 425, 99

McClintock, J. E., & Remillard, R. A. 2003 (astro-ph/0306213)

Maccarone, T. J., Gallo, E., & Fender, R. 2003, MNRAS, 345, L19

Middelberg, E., et al. 2004, A&A, 417, 925

Moran, E. C. 2000, New Astronomy Review, 44, 527

Oshlack, A. Y. K. N., Webster, R. L., & Whiting, M. T. 2001, ApJ, 558, 578

Osterbrock, D. E., & Pogge, R. W. 1985, ApJ, 297, 166

Pounds, K. A., Done, C., & Osborne, J. P. 1995, MNRAS, 277, L5

Pogge, R. W. 2000, New Astronomy Review, 44, 381

Readhead, A. C. S. 1994, ApJ, 426, 51

Reeves, J. N., Turner, M. J. L., Ohashi, T., & Kii, T. 1997, MNRAS, 292, 468

Reich, W., Fürst, E., Reich, P., Kothes, R., Brinkmann, W., & Siebert, J. 2000, A&A, 363, 141

Shepherd, M. C. 1997, Astronomical Society of the Pacific Conference Series, 125, 77

Siebert, J., Leighly, K. M., Laurent-Muehleisen, S. A., Brinkmann, W., Boller, T., & Matsuoka, M. 1999, A&A, 348, 678

Spergel, D. N., et al. 2003, ApJS, 148, 175

Stocke, J. T., Morris, S. L., Weymann, R. J., & Foltz, C. B. 1992, ApJ, 396, 487

Taylor, G. B., Frail, D. A., Berger, E., & Kulkarni, S. R. 2004, ApJL, 609, L1

Ulvestad, J. S., Antonucci, R. R. J., & Goodrich, R. W. 1995, AJ, 109, 81

Valtaoja, E., Lähteenmäki, A., Teräsranta, H., & Lainela, M. 1999, ApJS, 120, 95

Visnovsky, K. L., Impey, C. D., Foltz, C. B., Hewett, P. C., Weymann, R. J., & Morris, S. L. 1992, ApJ, 391, 560

Wang, T. G., Matsuoka, M., Kubo, H., Mihara, T., & Negoro, H. 2001, ApJ, 554, 233

Williams, R. J., Pogge, R. W., & Mathur, S. 2002, AJ, 124, 3042

Zhou, H., & Wang, T. 2002, Chinese Journal of Astronomy and Astrophysics, 2, 501

Zhou, H., Wang, T., Dong, X., Zhou, Y., & Li, C. 2003, ApJ, 584, 147 (Z03)